microbial biotechnology

Open Access

Transplantion of predominant *Lactobacilli* from native hens to commercial hens could indirectly regulate their ISC activity by improving intestinal microbiota

Lijuan Liu,† Zhou Zhou,† Yi Hong, Keyang Jiang, Lingzi Yu, Xiaochen Xie, Yuling Mi, Shu Jeffrey Zhu, Caiqiao Zhang and Jian Li*

Department of Veterinary Medicine, Zhejiang Provincial Key Laboratory of Preventive Veterinary Medicine, College of Animal Sciences, Zhejiang University, Hangzhou, 310058, China.

Summary

In poultry, HyLine (HL) Hens are known for their excellent laying performance. However, ZhenNing (ZN) Hens, a native chicken breed in China, are known for their unique flavour. The intestinal mucosa, which is the main organ for nutrient absorption, could affect livestock product quality. In ZN Hens' intestinal mucosa, we found more villus wrinkles, larger villus circumference and higher amino acid transporters mRNA abundance compared with HL Hens. Among three laying periods of ZN Hens, in the intestinal lumen, *Lactobacillus salivarius (L. sa.)*, *Lactobacillus agilis (L. ag.)* and *Lactobacillus aviarius* were the predominant species in the laying peak period. Furthermore, multiple-antibiotics feeding in ZN Hens and predominant *Lactobacillus* feeding in HL Hens suggested that these *Lactobacilli* could indeed increase villus wrinkles and improve intestinal absorption. In HL Hens, *L. sa.* + *L. ag.* treatment could promote organoids budding *in vitro*, and promote epithelial proliferation *in vivo*. Collectively, the unique intestinal mucosa morphology in ZN Hens was due to the high abundance of intestinal *L. sa.* and *L. ag.* Transplant these *Lactobacilli* to HL Hens could increase their intestinal probiotics abundance, fine adjust the intestinal stem cell function and promote the epithelial proliferation, in turn, increase villus winkles and mucosal absorption area.

Received 27 April, 2021; revised 22 August, 2021; accepted 25 August, 2021.
*For correspondence. E-mail: lijiannp@zju.edu.cn; Tel: 86-571-88982976; Fax: 86-571-88982976.
†These authors contributed equally to this work.
Microbial Biotechnology (2022) **15**(4), 1235–1252
doi:10.1111/1751-7915.13917

Introduction

The intestinal mucosa is the main organ that exerts nutrient absorption. For laying hens in the laying peak period, they have higher requirements for intestinal mucosal absorption (Gu *et al*., 2021). In hens with various breeds, laying performance and egg nutrition vary considerably. It is well known that HyLine (HL) Hens are famous for their excellent laying performance while compromise in flavour. On the other hand, ZhenNing (ZN) Hens, a native chicken breed of Zhejiang province in China, are known for their unique flavour and high nutrition while compromise in laying performance. In chickens, the rearing environment greatly affected gut length and function, contributing to the variation in feed intake among various breeds (Metzler-Zebeli *et al*., 2018). In pigs, small intestinal mucosal morphology (such as villus height, width, surface, etc.) differed sharply between native pig breeds (Iberian pigs) and lean pig strain, and these differences tended to disappear with age (Rubio *et al*., 2010). However, whether the intestinal mucosa is different between ZN Hens and HL Hens and how these morphological differ formed is worthy of being studied.

The gut microbiota is referred to as a forgotten organ and is recognised as an essential component of the intestinal ecosystem, contributing to nutrition absorption and disease resistance (O'Hara and Shanahan, 2006). Growing evidence has revealed that probiotics could improve product performance in the livestock and poultry industry. Firmicutes were the predominant phylum of the gut microbiota in the broiler (Mancabelli *et al*., 2016). However, due to the difference in diet and/or the intensive use of antibiotics, higher *Bacteroidetes* and *Proteobacteria* levels appeared in the free-range chicken (Mancabelli *et al*., 2016). In avian, supplied laying hens with *Bacillus subtilis* could improve their egg production and eggshell quality (Abdelqader *et al*., 2013; Ribeiro *et al*., 2014). In Japanese quail, dietary supplementation with probiotics containing *Lactobacillus* (*L*.) *casei* and *L. rhamnosus* could increase egg weight and improve yolk colour, albumen height and haugh unit (Lokapirnasari *et al*., 2019). Recently, faecal microbiota transplantation (including *L. frumenti*, *L. gasseri*) from a Chinese native pig breed to early weaning piglets was demonstrated to prevent weaning stress-induced diarrhoea (Hu *et al*.,

2018). However, intestinal microorganisms differ sharply among the various breeds of chickens. Whether transplanted the predominant probiotic from native hens to commercial laying hens can regulate their intestinal mucosal absorption and further improve egg quality and the flavour is worth studying.

The function of intestinal mucosal absorption relies on mucosal renewal, which depends on the proliferation and differentiation of intestinal stem cells (ISCs) in the crypt's bottom region. A large number of studies have shown that *Lactobacillus* could regulate the activity of ISCs, thereby affecting the structure and function of the intestinal mucosa. Recently, *L. plantarum* was demonstrated to increase the ratio of villus height and crypt depth in the duodenum and jejunum of chickens (Xu *et al.*, 2020). *L. plantarum* IS-10506 was demonstrated to increase the size of the Lgr5- and Bmi1-expressing ISCs pool and further relieve intestinal mucosal injury in rats (Athiyyah *et al.*, 2018; Lee *et al.*, 2018). *Lactobacillus reuteri* could maintain the number of $Lgr5^{+}$ cells and stimulate intestinal epithelial proliferation by increasing the expression of R-spondins and thus activating the Wnt/β-catenin pathway (Wu *et al.*, 2020). However, between HL Hens and ZN Hens, whether the differential intestinal flora could give rise to the differential ISCs activities and further induce the differential product performance is worth clarifying.

In this study, we analysed the intestinal mucosal differences between ZN Hens and HL Hens. Moreover, the relationship between intestinal flora and intestinal mucosa was further investigated by multiple-antibiotics and predominant *Lactobacillus* feeding. Finally, the possible mechanism of action for *Lactobacillus* on intestinal mucosa was explored.

Results

Morphological and functional difference of intestinal mucosa between ZN Hens and HL Hens

For analysing the morphological and functional difference of intestinal mucosa between ZN Hens and HL Hens in the laying peak period, the H&E staining, AB-PAS staining and qPCR were performed. Compared with HL Hens, the duodenum of ZN Hens presented more villus wrinkles (Fig. 1A, B and E, black arrows, more than 3.7 folds, P-value < 0.001), larger villus circumference (Fig. 1F, larger by 43.67%, P-value = 0.007), higher density of goblet cells (Fig. 1C, D and G, higher by 74.09%, P-value < 0.001) and higher transcription level of *MUC2* mRNA (Fig. 1H, higher by 137.67%, P-value = 0.006). The mRNA transcription assay of amino acid transporter in duodenum (Fig. 1I–L) revealed that, compared with HL Hens, higher *PepT1* (by 47 folds, P-value < 0.001), B^0AT (by 104 folds, P-value < 0.001), $b^{0,+}AT$ (by 17 folds, P-value < 0.001) and *EAAT3* (by 30 folds, P-value < 0.001) were present in ZN Hens. Parallelly, as shown in Table S1, significant higher level of Cys (by 149.3%, P-value < 0.001), Leu (by 107.2%, P-value < 0.001), Lys (by 61.25%, P-value = 0.012) and His (by 67.55%, P-value = 0.005) were present in albumen of ZN Hens when compared with HL Hens.

For illustrating the profile of the morphological changes among three laying periods in ZN Hens, the number of villus wrinkles was analysed. As shown in Fig. 2, compared with D150 (150-day-old, pre-laying peak period) and D580 (580-day-old, post-laying peak period), the number of villus wrinkles in D280 (280-day-old, laying peak period) was the most, especially for the duodenum. In the laying peak period, the duodenal villus wrinkles amount was, respectively, higher by 39.58% (P-value = 0.003) and 214.06% (P-value < 0.001) than jejunum and ileum.

Intestinal macrobiotic assay among three laying periods in ZN Hens

For exploring the mechanism that mucosal morphology of ZN Hens changes among three laying periods, the intestinal content was collected and sequenced 16S rRNA gene V3-V4 region. In total, 1 275 223 quality-checked sequences were clustered into 2,981 OTUs at 97% sequence similarity with an average Good's coverage of 99.71 ± 0.25% in all the samples. In D280, the number of exclusive OTUs (Fig. 3A) was the lowest among three laying periods, and total observed OTUs (Fig. 3B) were lower than D150 (P-value = 0.021) and D580 (P-value < 0.001). The α-diversity analysis showed that Chao1 richness estimate (Fig. 3C) and Shannon diversity index (Fig. 3D) in the D280 group was, respectively, lower than D150 (P-value = 0.007 and 0.027) and D580 (P-value < 0.001), which indicated that the richness and diversity of the intestinal macrobiotic were significantly decreased in the D280 group. Interestingly, the β-diversity analysis presented a distinct clustering of the intestinal macrobiotic composition among three laying periods. The PCoA (Fig. 3E) and NMDS (Fig. 3F) showed a significant separation in bacterial community composition among the three laying periods. The Bray–Curtis index showed that the microbial communities were significantly different in the D280 than the D150 (P-value = 0.028) and D580 (P-value = 0.005).

When assessing the microbial composition at phylum-level, it suggested that the Firmicutes were the predominant phyla in the intestinal content (Fig. 4A and B). The relative abundance of Firmicutes in D280 group (95.81%) was higher than D150 groups (71.18%) and D580 groups (48.09%). The assay of microbial composition at genus-level (Fig. 4C and D) further clarified that

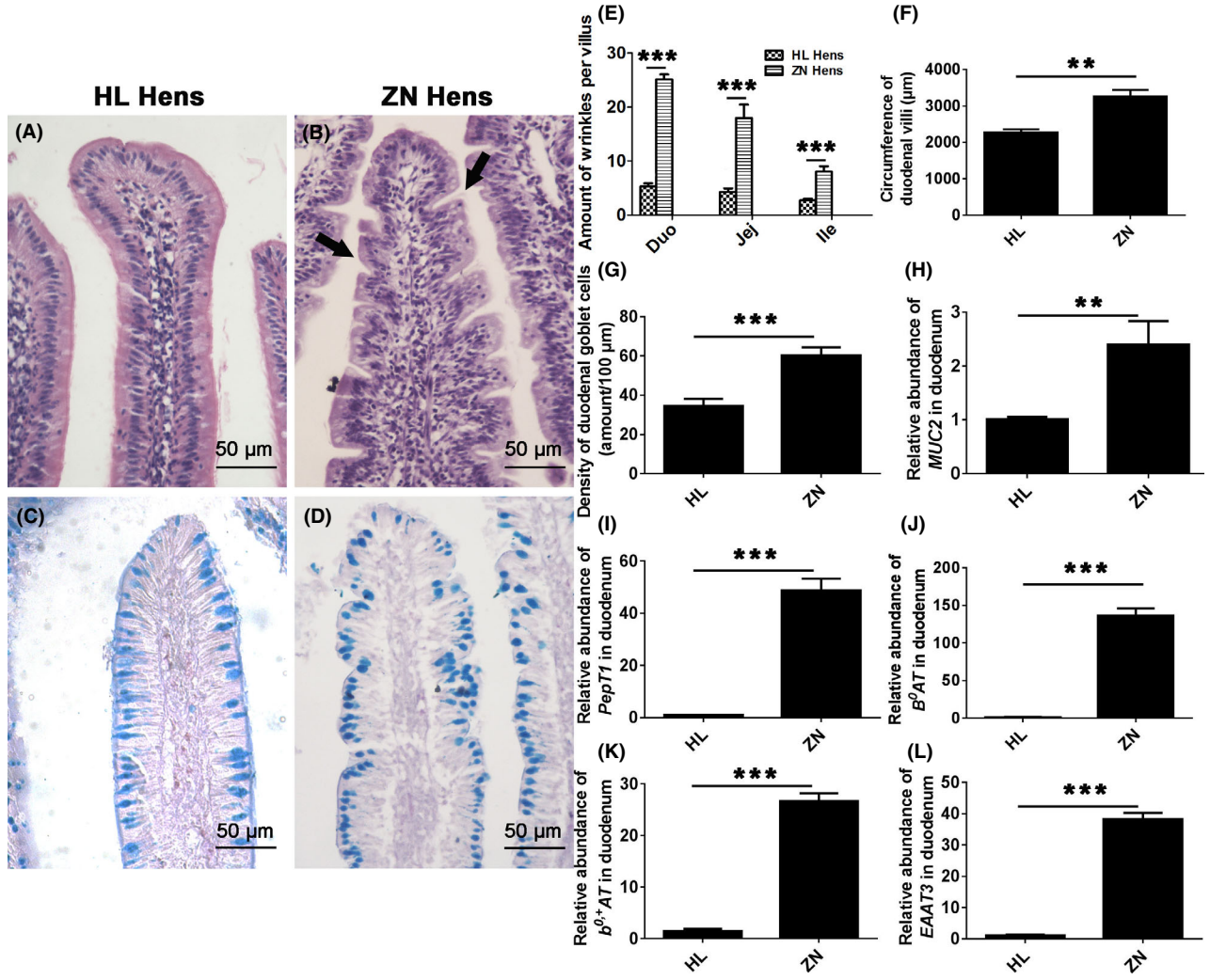

Fig. 1. Intestinal villus morphological and functional analysis between HL Hens and ZN Hens in the laying peak period.
A and B. H&E staining results show more wrinkles (black arrows) appeared in the duodenal villus of ZN Hens.
C and D. AB-PAS staining results show more goblet cells in the duodenal villus of ZN Hens.
Histograms represent the statistical results of wrinkles amount (E), villus circumference (F), goblet cell density (G) and mRNA abundance of goblet cell marker *MUC2* (H) and mainly amino acid transporter (I–L) in duodenum between HL Hens and ZN Hens. The data were expressed as mean ± standard deviation, $n = 5$. ***P*-value <0.01. ****P*-value <0.001. Duo, duodenum; Ile, Ileum; Jej, jejunum. Scale bar = 50 μm.

the relative abundance of *Lactobacillus* was the highest in D280 group (91.26%) and was higher than D150 group (58.62%) and D580 group (21.18%). Heatmap of microbial composition at species-level (Fig. 4E) further illustrated that the higher *Lactobacillus* and lower pathogenic bacteria appeared in D280 group. Among the top ten enriched species in D280 group, five were *Lactobacillus* (Fig. 4F). As shown in Fig. 4G–K, the result of Kruskal-Wallis test showed that *Lactobacillus agilis* (*L. ag.*, *P*-value = 0.003) and *L. intestinalis* (*P*-value = 0.002) has significantly different abundances among the three laying periods. Then, the result of pairwise-Wilcoxon test confirmed that the abundance of *L. ag.* between D150 and D280 was significant difference (adjusted *P*-value = 0.005), the abundance of *L. intestinalis* between D280 and D580 was significant difference (adjusted *P*-value = 0.004). However, *Lactobacillus salivarius* (*L. sa.*) and *Lactobacillus aviarius* (*L. av.*) were decreased with age without statistical significance.

Effect of multiple-antibiotics feeding on the intestinal mucosa of ZN Hens

For identifying whether intestinal flora could regulate the mucosal structure, the ZN Hens in the laying peak period were fed with multiple-antibiotics (Ampicillin, Neomycin, Vancomycin, and Metronidazole) for five consecutive

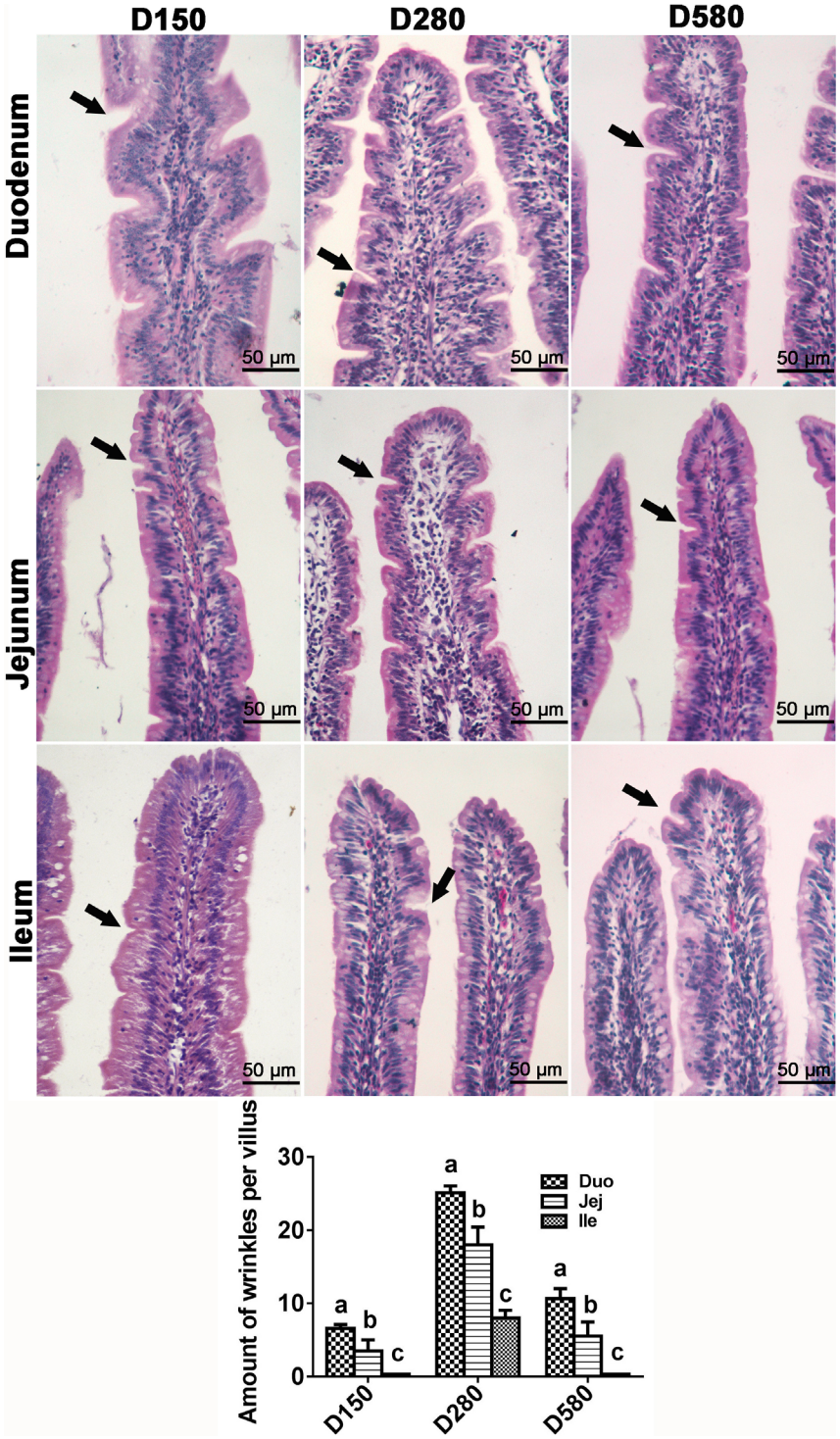

Fig. 2. Villus morphological analysis in duodenum, jejunum and ileum among three laying periods in ZN Hens. H&E staining results show a large number of villus wrinkles (black arrows). Histogram represents the statistical results of villus wrinkles amount among three laying periods in ZN Hens. The data were expressed as mean ± standard deviation, $n = 5$. The columns with no common letters are significant differences (P-value <0.05) within each laying period. Duo, duodenum. Jej, jejunum. Ile, Ileum. D150, 150-day-old, pre-laying peak period. D280, 280-day-old, laying peak period. D580, 580-day-old, post-laying peak period. Scale bar = 50 μm

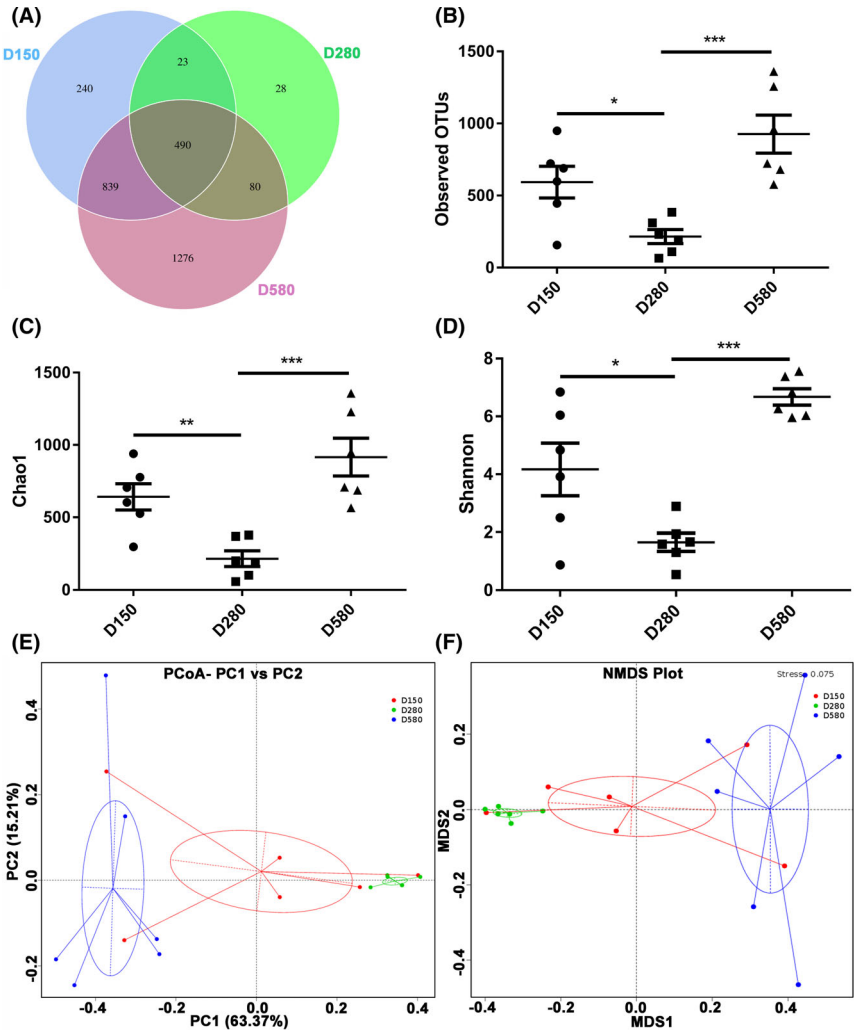

Fig. 3. The richness and diversity assays of intestinal microbiota among three laying periods in ZN Hens.
A. Venn diagram.
B. Observed OTUs.
C. Chao1 richness estimate.
D. Shannon diversity index.
E. Principal Coordinates Analysis, PCoA.
F. Nonmetric Multidimensional Scaling, NMDS.
D150, 150-day-old, pre-laying peak period. D280, 280-day-old, laying peak period. D580, 580-day-old, post-laying peak period. **P*-value <0.05; ***P*-value <0.01; ****P*-value < 0.001. $n = 6$.

days to ablate intestinal microbiota. First, the CFUs assay of intestinal content (Fig. 5A) showed that gut bacteria in multiple-antibiotics treated hens were dramatically reduced. In expectation, after multiple-antibiotics feeding, observed OTUs (Fig. 5B, *P*-value < 0.001), Chao1 richness estimate (Fig. 5C, *P*-value < 0.001) and Shannon diversity index (Fig. 5D, *P*-value < 0.001) decreased markedly when compared with the control group. The assay of microbial composition at genus- and species-level (Fig. 5E and F) showed that, due to multiple-antibiotics feeding, there were less abundance of *Lactobacillus* and more abundance of *Escherichia coli* in intestinal lumen. The heatmap of microbial composition at species-level (Fig. 5G) further clarified that decreased *Lactobacillus* includes *L. sa.*, *L. ag.* and *L. av.*

After multiple-antibiotics feeding, the mucosal structure and function in the duodenum were analysed to illustrate intestinal microbiota's influence on the intestinal mucosa. Upon multiple-antibiotics feeding, the number of duodenal villus wrinkles (Fig. 6A and C), the duodenal goblet cells density (Fig. 6B and D) and the *MUC2* mRNA abundance (Fig. 6E) were, respectively, decreased by 15.54% (*P*-value = 0.027), 51.24% (*P*-value < 0.001)

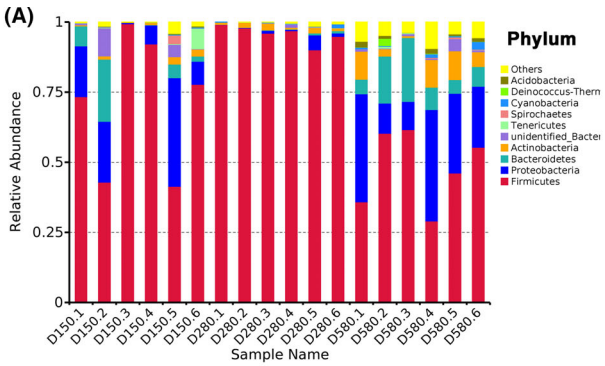

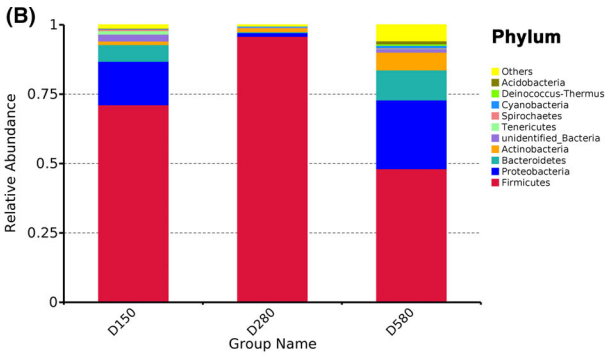

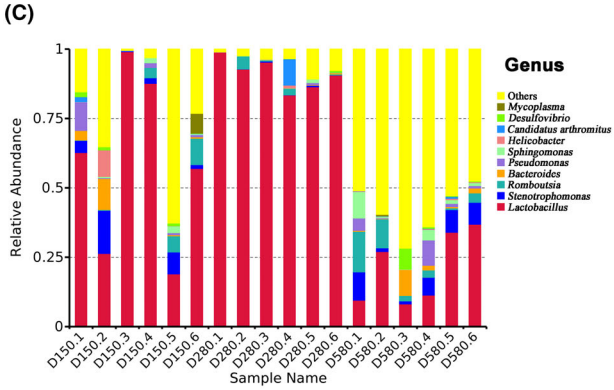

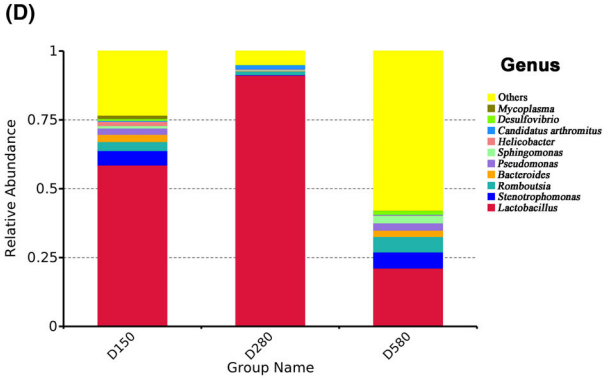

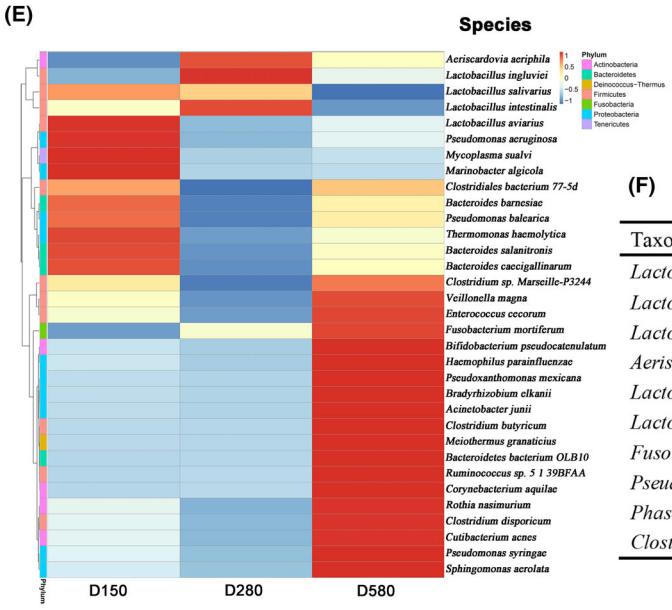

(F)

Taxonomy	D150	D280	D580
Lactobacillus aviarius	0.142989	0.042034	0.065217
Lactobacillus intestinalis	0.01544	0.02996	0.003315
Lactobacillus salivarius	0.016337	0.015129	0.007587
Aeriscardovia aeriphila	0.001099	0.012642	0.006758
Lactobacillus ingluviei	0.00082	0.004029	0.001717
Lactobacillus agilis	0.000723	0.004029	0.001291
Fusobacterium mortiferum	0.000307	0.001511	0.003159
Pseudomonas aeruginosa	0.015316	0.001172	0.004588
Phaseolus vulgaris	0.000046	0.001076	0.000023
Clostridium sp. Marseille-P3244	0.004355	0.000829	0.005948

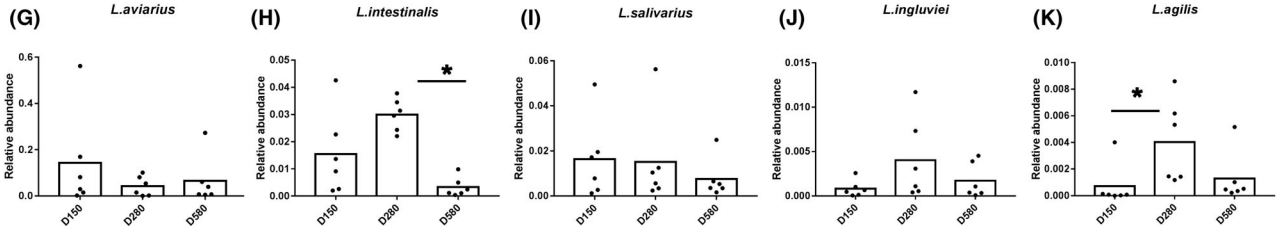

Fig. 4. The assay of microbial composition at phylum-, genus- and species-level in intestinal lumen from three laying periods in ZN Hens.
A and B. Histograms represent the top 10 phyla in each sample (A) and each group (B).
C and D. Histograms represent the top 10 genera in each sample (C) and each group (D).
E. Heatmap of microbial composition at species-level in each group.
F. The relative abundance of top 10 species in each group.
G–K. Changes in the relative abundance of five indigenous *Lactobacillus* species in the small intestine among three laying periods. Kruskal–Wallis test was performed to analyse the statistical significance among various groups, followed by the pairwise-Wilcoxon test (with *P*-value adjusted by FDR method of Benjamini and Hochberg). **P*-value <0.05. *n* = 6. D150, 150-day-old, pre-laying peak period. D280, 280-day-old, laying peak period. D580, 580-day-old, post-laying peak period.

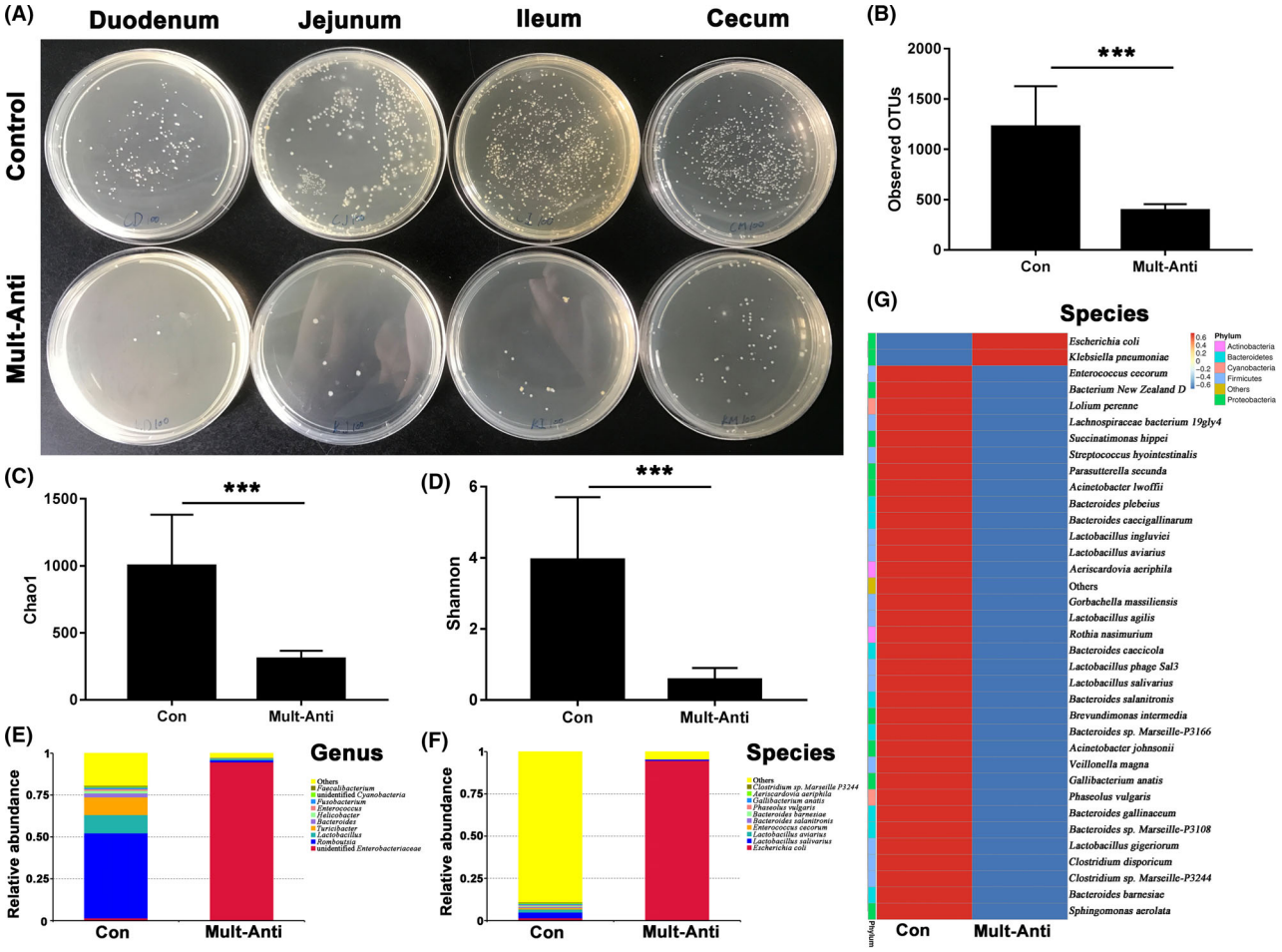

Fig. 5. Intestinal microbiota assay in ZN Hens after multiple-antibiotics feeding. Multiple-antibiotics (Ampicillin, Neomycin, Vancomycin, and Metronidazole) were fed in ZN Hens during the laying peak period for five consecutive days.
A. CFUs assay of intestinal content.
B. Observed OTUs.
C. Chao1 richness estimate.
D. Shannon diversity index.
E. The assay of microbial composition at genus-level.
F and G. The assay of microbial composition at species-level.
****P*-value <0.001. *n* = 6. Con, control. Mult-Anti, multiple-antibiotics.

and 59.25% (*P*-value = 0.001) when compared with the control group. Moreover, less abundance of duodenal *PepT1* (decreased by 74.35%, *P*-value < 0.001) and B^0AT (decreased by 43.75%, *P*-value = 0.001) were detected upon antibiotic feeding (Fig. 6F–I).

Effect of predominant Lactobacillus *feeding on the duodenal mucosa of HL Hens*

To determine if the predominant *Lactobacillus* screened from ZN Hens (the breed with more villus wrinkles) could

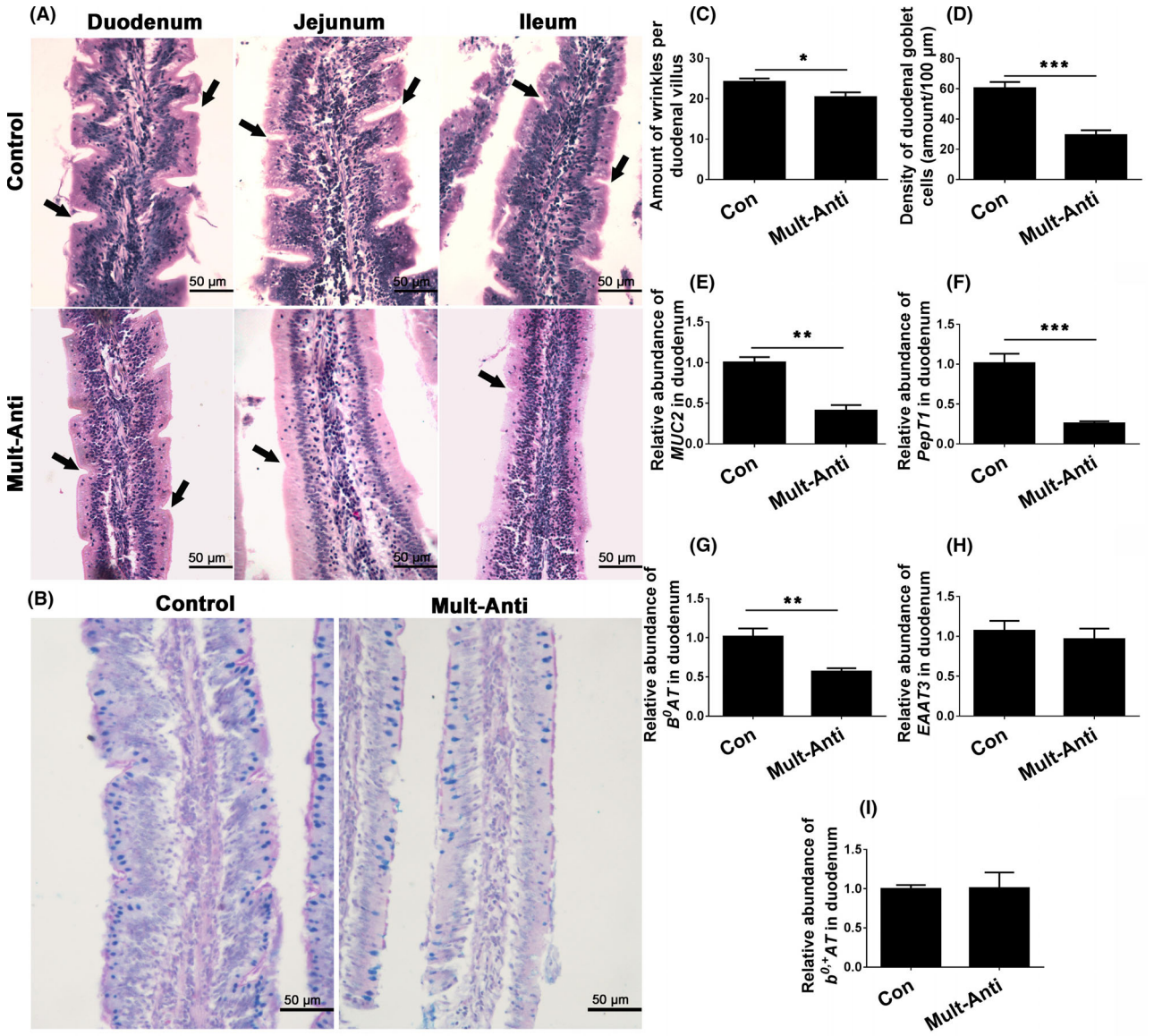

Fig. 6. Changes of intestinal mucosal morphology and absorption function after multiple-antibiotics feeding in ZN Hens during the laying peak period.
A. H&E staining of the intestinal villus in the control and multiple-antibiotics feeding groups, black arrows indicate the villus wrinkles, scale bar = 50 μm.
B. AB-PAS staining of the intestinal villus in the control and multiple-antibiotics feeding groups, scale bar = 50 μm.
Histograms represent the changes of villus wrinkles amount (C), goblet cells density (D) and mRNA abundance of *MUC2* (E) and mainly amino acids transporters (F–I) in duodenum after multiple-antibiotics feeding. The data were expressed as mean ± standard deviation, $n = 5$. **P*-value <0.05. ***P*-value <0.01; ****P*-value <0.001. Con, control; Mult-Anti, multiple-antibiotics.

regulate duodenal mucosal morphology in HL Hens (the breed with fewer villus wrinkles), the predominant *Lactobacillus* were fed in HL Hens for 30 consecutive days. As shown in Fig. 7A and F, in the group of *L. sa.* + *L. ag.* and *L. sa.* + *L. av.*, the wrinkles amount were more than that in the control group by 48.12% and

Fig. 7. Effect of predominant *Lactobacillus* feeding on duodenal villus morphology and proliferation in HL Hens.
A. H&E staining results show more wrinkles (black arrows) appeared upon *Lactobacillus* feeding, scale bar = 50 μm.
B. AB-PAS staining results show more goblet cells in the villus upon *Lactobacillus* feeding, scale bar = 50 μm.
C and D. Immunostaining and Western Blot assay of duodenal PCNA protein upon *Lactobacillus* feeding, scale bar = 100 μm.
Histograms represent the changes of PCNA protein levels (E), villus wrinkles amount (F), villus circumference (G), goblet cell density (H) and the mRNA abundance of *PepT1* (I), B^0AT (J), *EAAT3* (K) and $b^{0,+}AT$ (L) upon *Lactobacilli* co-feeding, $n = 5$. The columns with no common letters are significant differences (*P*-value <0.05) among various treatments. Con, control. *L. sa., L. salivarius. L. ag., L. agilis. L. av., L. aviarius.*

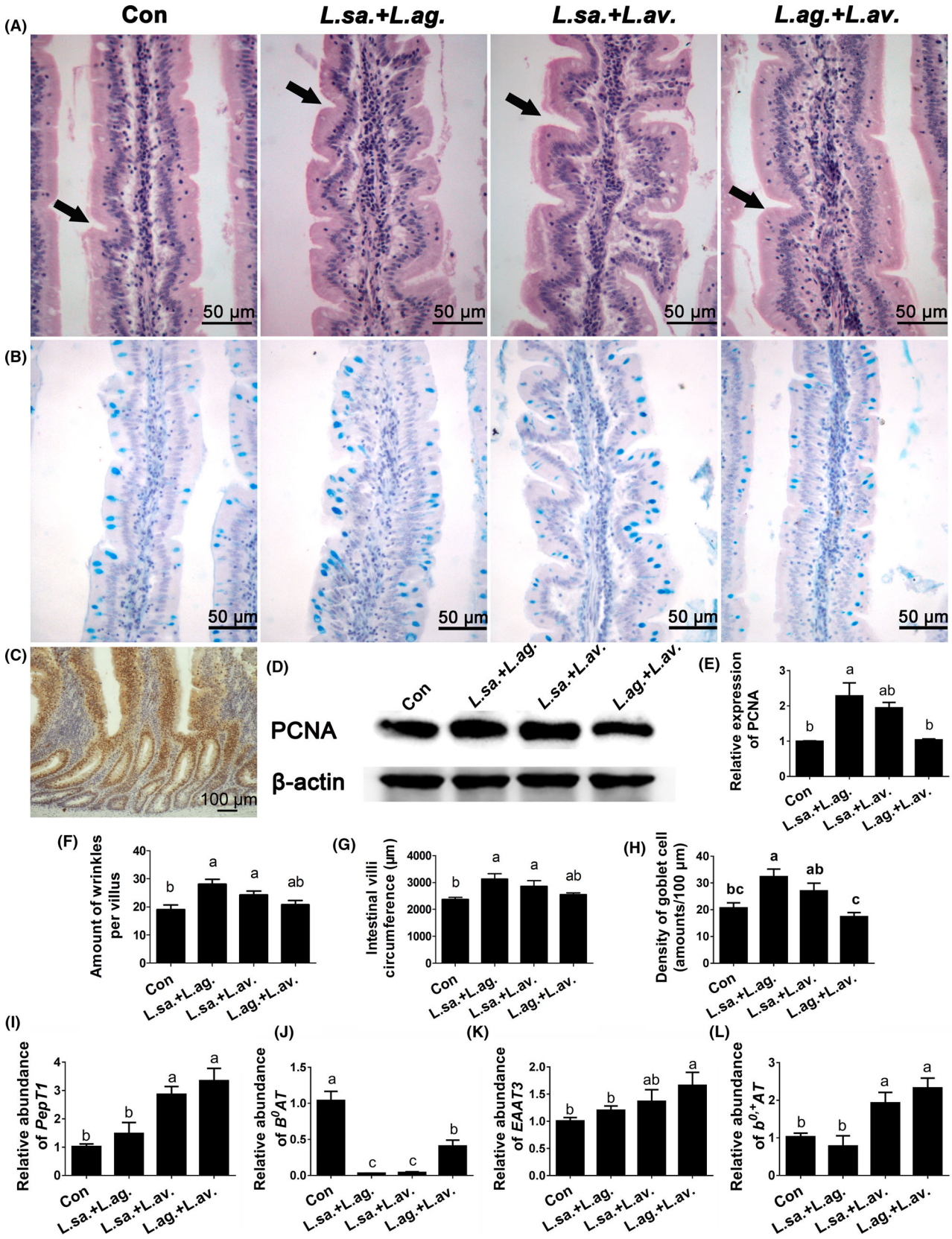

27.94% (*P*-value = 0.002 and 0.028), thus give rise to larger absorption area (villus circumference was larger by 32.60% and 21.15% than the control group, *P*-value = 0.012 and 0.037, Fig. 7G). Meanwhile, the mRNA abundance of *PepT1* (Fig. 7I) and *EAAT3* (Fig. 7K) in duodenum were increased by 19.22% to 227.26% after *Lactobacilli* co-feeding. In addition, as shown in Fig. 7B and H, goblet cell density in *L. sa.* + *L. ag.* group was higher by 56.57% (*P*-value = 0.001). To explore whether the increasing wrinkles amount is the result of enhanced epithelial proliferation, the PCNA protein (proliferating cell nuclear antigen) expression was analysed. As shown in Fig. 7C–E, the PCNA positive cells were located at the crypt and villus base, and the PCNA protein levels in *L. sa.* + *L. ag.* group were higher than the control group by 128.41% (*P*-value = 0.029).

Effect of predominant Lactobacillus *feeding on intestinal microbiota of HL Hens*

For illustrating the possible mechanism of action for *Lactobacillus* on the intestinal mucosa, the intestinal microbiota was assayed by 16S rRNA gene sequencing after feeding predominant *Lactobacillus* in HL Hens (laying peak period). In *L. sa.* + *L. ag.* group, the exclusive OTUs numbers was the highest among various groups (Fig. 8A). However, the total observed OTUs in *L. sa.* + *L. ag.* group was significantly lower than the control group (Fig. 8B, *P*-value < 0.001). When compared with the control group, as shown in Fig. 8C and D, there appeared lower Chao1 richness estimate in groups of *L. sa.* + *L. ag.* (*P*-value = 0.023), *L. sa.* + *L. av.* (*P*-value < 0.001) and *L. ag.* + *L. av.* (*P*-value < 0.001), and lower Shannon diversity index in *L. sa.* + *L. av.* group (*P*-value = 0.042).

The assay of microbial composition at phylum-level (Fig. 9A) indicating that Firmicutes were the predominant phyla in the intestinal content, no matter fed with *Lactobacillus* or not. When assessing the microbial composition at genus-level, it further clarified that the relative abundance of *Lactobacillus* was higher in *L. sa.* + *L. ag.* and *L. sa.* + *L. av.* groups (Fig. 9B). Heatmap of microbial composition at species-level (Fig. 9C, red box) showed that, compared with the control group, more abundance of probiotics species (such as *Bifidobacterium*, *Clostridium butyricum*, *L. casei*, etc.) and less abundance of pathogenic microorganism (such as *Clostridium disporicum*) appeared in *L. sa.* + *L. ag.*

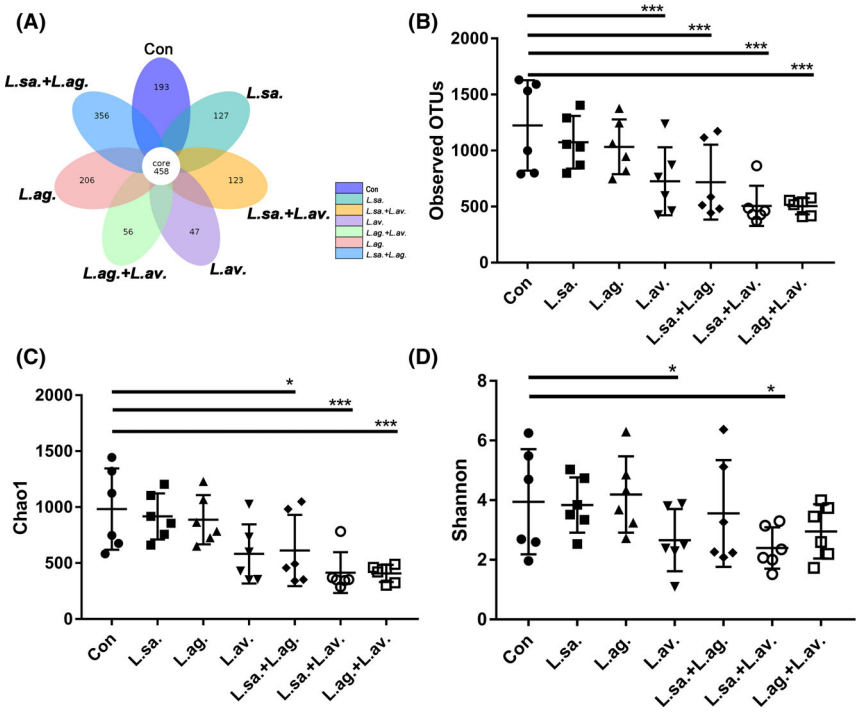

Fig. 8. The richness and diversity assays of intestinal content from HL Hens after *Lactobacillus* feeding.
A. Venn diagram.
B. Observed OTUs.
C. Chao1 richness estimate.
D. Shannon diversity index.
**P*-value <0.05; ****P*-value <0.001. *n* = 6. Con, control. *L. sa., L. salivarius. L. ag., L. agilis. L. av., L. aviarius.*

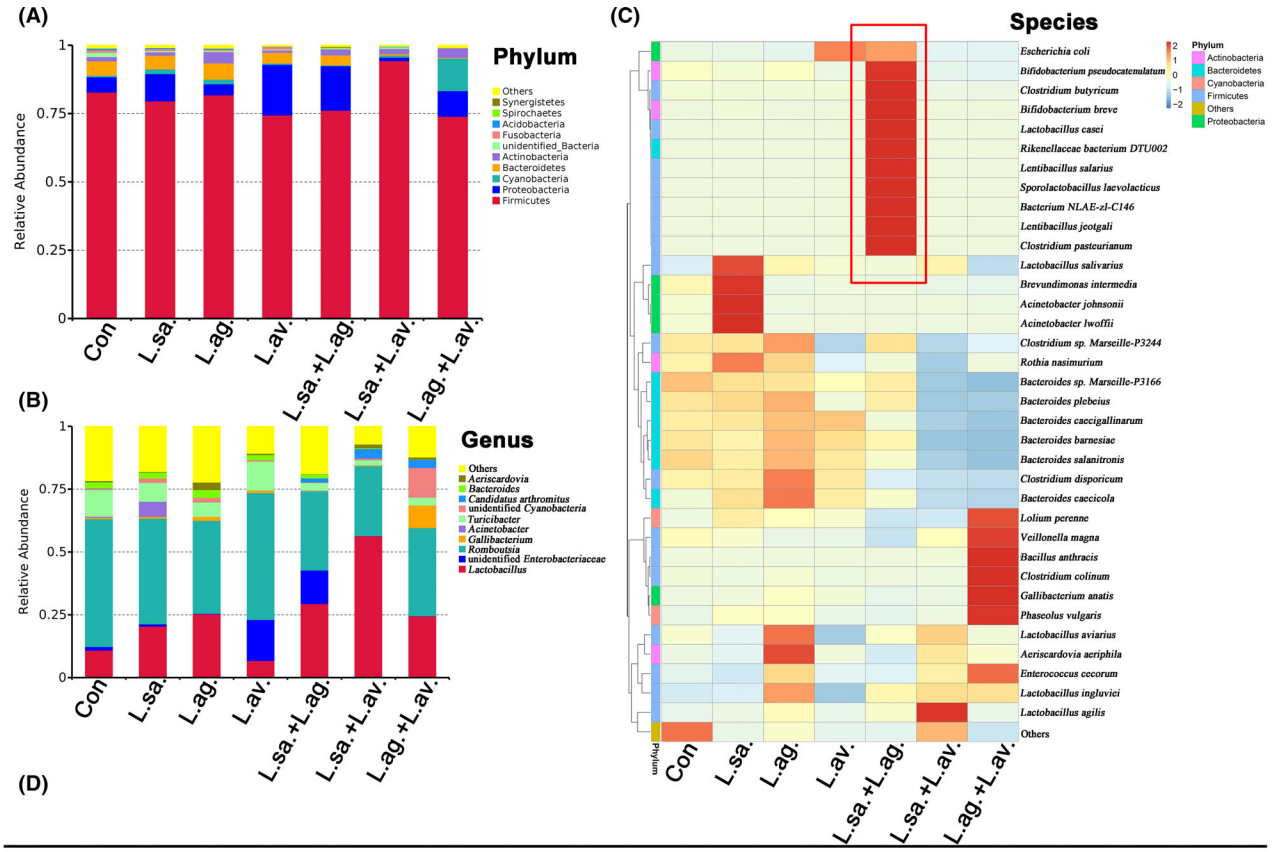

L. sa. + L. ag.		*L. sa. + L. av.*		*L. ag. + L. av.*	
Others	0.696701	**Others**	0.825481	**Others**	0.696585
Escherichia coli	0.1337	*Lactobacillus salivarius*	0.062102	*Phaseolus vulgaris*	0.090616
Lactobacillus salivarius	0.048634	*Lactobacillus aviarius*	0.029844	*Gallibacterium anatis*	0.089763
Lactobacillus aviarius	0.018276	*Enterococcus cecorum*	0.019316	*Enterococcus cecorum*	0.036478
Sporolactobacillus laevolacticus	0.009095	*Aeriscardovia aeriphila*	0.014835	*Lactobacillus salivarius*	0.024265
Enterococcus cecorum	0.006747	*Lactobacillus agilis*	0.014421	*Lactobacillus aviarius*	0.015328
Lactobacillus ingluviei	0.006216	*Lactobacillus ingluviei*	0.007376	*Aeriscardovia aeriphila*	0.008287
Clostridium Marseille	0.004841	*Phaseolus vulgaris*	0.006241	*Lactobacillus ingluviei*	0.007716
Lactobacillus agilis	0.004278	*Veillonella magna*	0.003599	*Veillonella magna*	0.007521
Bacteroides barnesiae	0.003649	*Gallibacterium anatis*	0.002791	*Bacillus anthracis*	0.00398

Fig. 9. The assay of microbial composition at phylum-, genus- and species-level in intestinal lumen from HL Hens after *Lactobacillus* feeding. Histograms represent the top 10 phyla (A) and the top 10 genera (B) in each group.
C. Heatmap of microbial composition at species-level in each group, red box shows the probiotics species with more abundant.
D. Top 10 abundance species in *L. sa.* + *L. ag.*, *L. sa.* + *L. av.* and *L. ag.* + *L. av.* groups. Con, control. *L. sa., L. salivarius. L. ag., L. agilis. L. av., L. aviarius*. $n = 6$.

group. As listed in Fig. 9D, *Lactobacillus* accounts for a relatively large proportion among the top ten enriched species, especially for the more abundance of *L. sa.*, *L. ag.* and *L. av.* in the *L. sa.* + *L. ag* feeding group.

Effect of predominant Lactobacillus *treatment on ISCs activity*

In vitro, HL Hens' crypt organoids were treated with predominant *Lactobacilli*. As shown in Fig. 10A, at 24 h of treatment, larger organoids size and more budding structures appeared in the *L. sa.* + *L. ag.* and *L. sa.* + *L. av.* groups when compared with the control group. At 48 h of treatment, the epithelial layer of organoids was further thickened. Moreover, the Western Blot assay of ISC marker (Fig. 10C and D) showed that, after 48 h of *L. sa.* + *L. av.* treatment, Lgr5 protein expression in organoids was up-regulated by 124.9% (*P*-value = 0.009) than the control group. The proliferation activity assay showed that organoids' EdU^+ cell density in *L. sa.* + *L.*

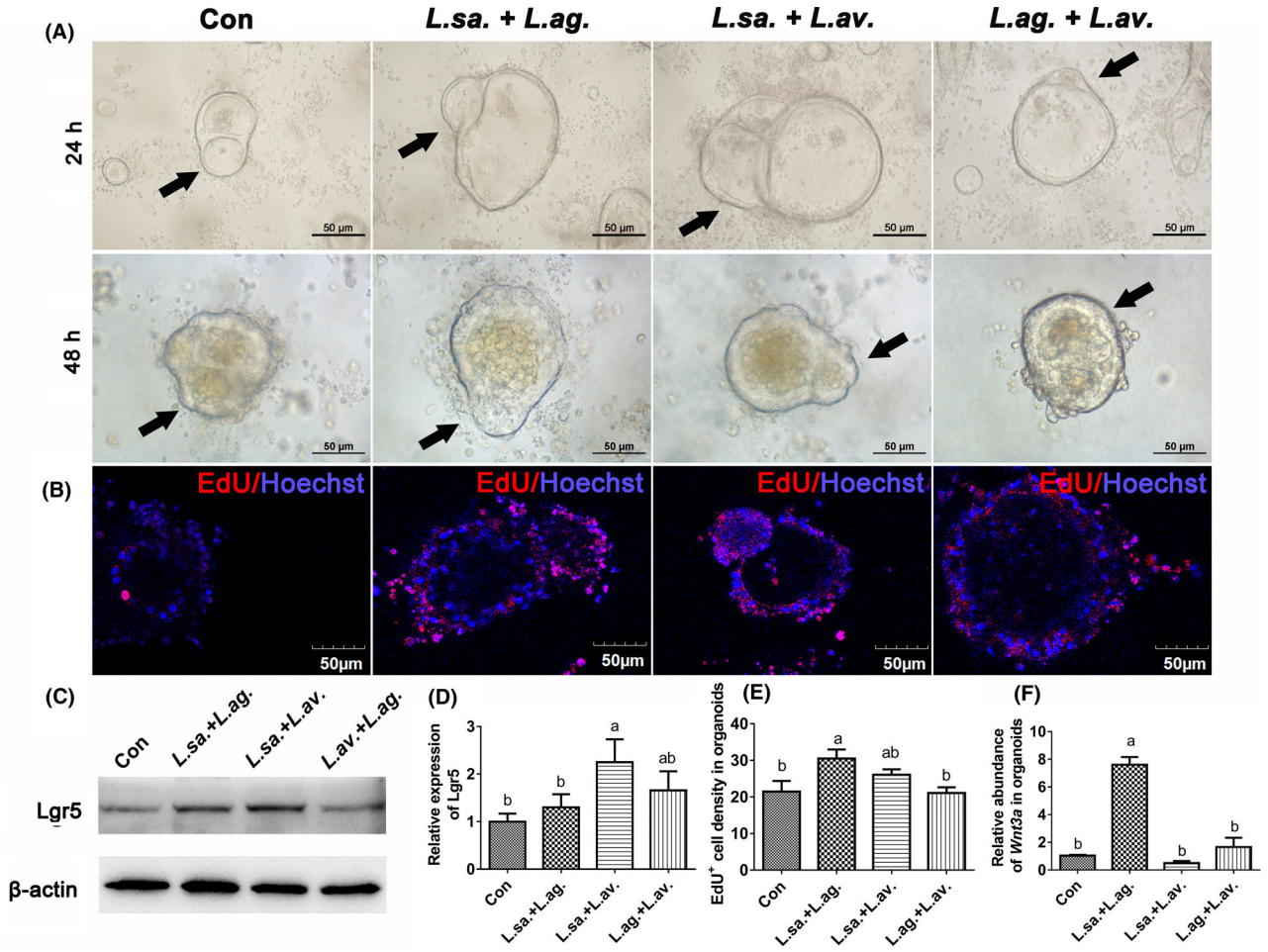

Fig. 10. Effect of predominant *Lactobacilli* treatment on crypt organoids *in vitro*. *Lactobacilli* treatment could promote the organoids budding (A, black arrows).
B. EdU incorporation assay on organoids, which treated with *Lactobacilli* for 48 h, red fluorescence indicated the EdU^+ cell.
C. The Western Blot assay of Lgr5 protein in organoids which treated with *Lactobacilli* for 48 h. Histograms represent the changes of Lgr5 protein levels (D), EdU^+ cell density (E) and the relative abundance of *Wnt3a* mRNA (F) in organoids, which treated with *Lactobacilli* for 48 h. The data were expressed as mean ± standard deviation, $n = 5$. The columns with no common letters are significantly different (P-value <0.05) among various groups. Con, control. *L. sa., L. salivarius. L. ag., L. agilis. L. av., L. aviarius*. Scale bar = 50 μm.

ag. groups (48 h of treatment) was higher by 41.85% (P-value = 0.009) than the control group (Fig. 10B and E). Besides, the *Wnt3a* mRNA abundance in organoids of *L. sa*. + *L. ag*. group (48 h of treatment) was higher by 6.29 fold (P-value < 0.001) than the control group (Fig. 10F).

To further confirm the influence of *L. sa*. + *L. ag*. co-feeding on ISCs of HL Hens *in vivo*, the location and expression assays of Lgr5 protein were analysed. Immunofluorescence staining showed that, in HL Hens, Lgr5 positive cells presented wedge-shaped and were located at the crypt's bottom (Fig. 11A, white arrows). After feeding of *L. sa*., *L. ag*. and *L. sa*. + *L. ag*. in HL Hens, as shown in Fig. 11B and C, the expression of crypt Lgr5 in *L. sa*. + *L. ag*. group were decreased by 68.8% (P-value = 0.030) than the control group.

Discussion

It is well known that the absorption capacity is dependent on the mucosal surface area and the activities of enterocytes. In this study, compared with HL Hens, more villus wrinkles and larger villus circumference were present in ZN Hens. Especially, the duodenal villus' wrinkles of ZN Hens were the highest in the laying peak period among three laying periods. Hence, we speculated that the unique mucosal morphology in the laying peak period was closely related to ZN Hens' unique flavour and high nutrition. Interestingly, Shang *et al*. (2018) found that the chicken intestinal mucosal mucin secretion and epithelial cell turnover rate increased upon microorganism's presence and further demonstrated that age is one of the most important factors influencing the intestinal

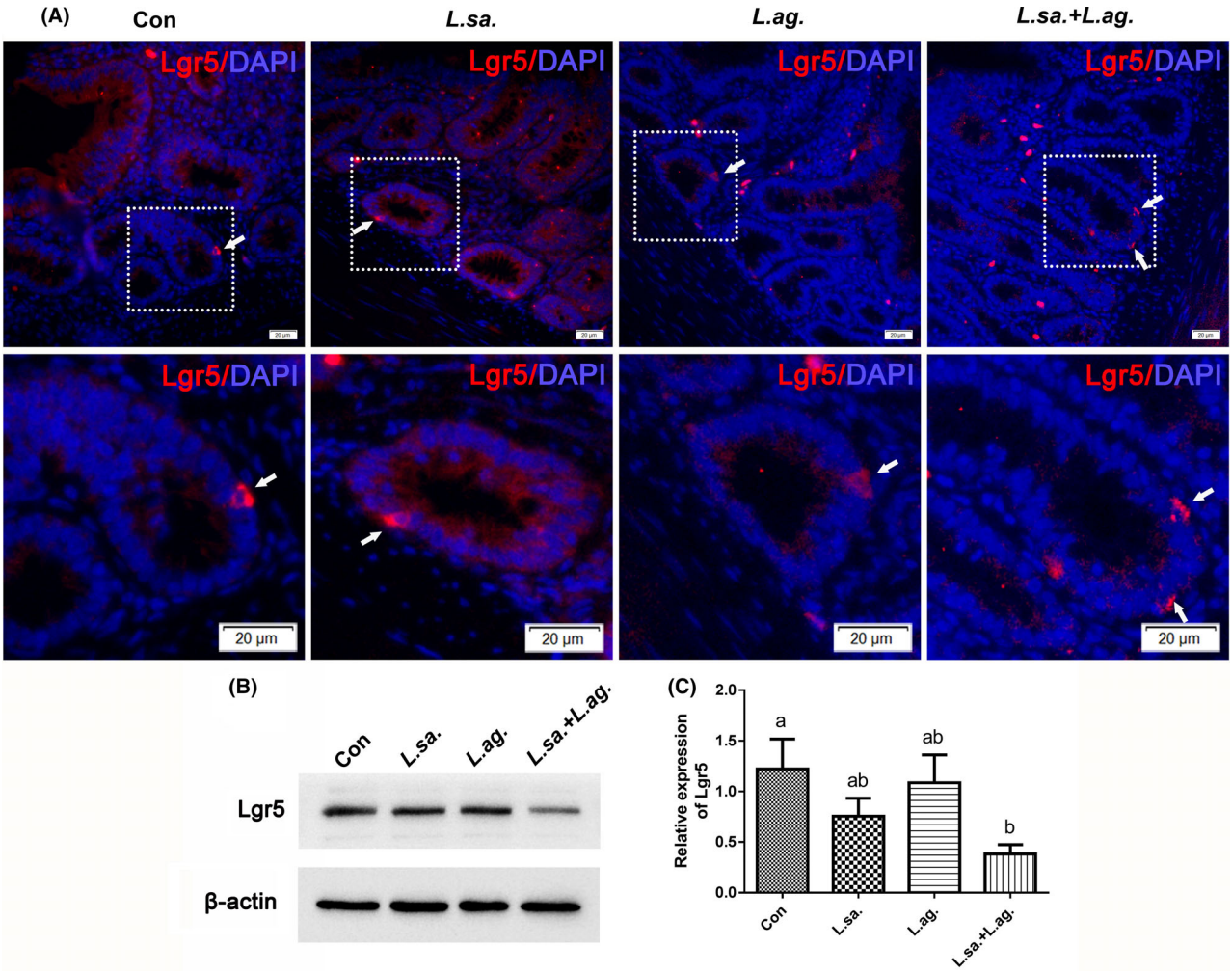

Fig. 11. Effect of predominant *Lactobacillus* treatment on ISCs activity.
A. The immunofluorescent staining of Lgr5 protein in the duodenum. The below panel shows an enlarged image of the boxed areas on the above. White arrows indicate $Lgr5^{+}$ ISC, Scale bar = 20 μm.
B. The Western Blot assay of Lgr5 protein in the duodenal crypt after *Lactobacillus* feeding.
C. Histogram represents the statistical results of relative expression of Lgr5 protein in the crypt, $n = 5$. The columns with no common letters are significant differences (P-value <0.05) among various treatments. Con, control. *L. sa., L. salivarius. L. ag., L. agilis*.

macrobiotic composition. Furthermore, in the current study, upon multiple-antibiotics feeding in ZN Hens, the number of duodenal villus wrinkles, the duodenal goblet cells density and the mRNA transcription of *MUC2, PepT1* and B^0AT were decreased remarkably. Similarly, the study on germ-free mice confirmed that the enteric microbiota could significantly increase Paneth cell numbers, though it does not appear to regulate jejunal ISC directly (Schoenborn *et al*., 2019). Besides, Lee *et al*. (2018) suggested that antibiotic feeding could reduce the Paneth cells' granules and the number of goblet cells in mice's intestine. These indicated that the gut flora was closely related to the unique mucosal morphology in ZN Hens.

Next, we sought to determine the possible pathway that causes unique mucosal morphology to appear in ZN Hens at the laying peak period. In the current study, from intestinal content among three laying periods of ZN Hens, 16S rRNA gene sequencing was performed. In the laying peak period, five *Lactobacillus* species (including *L. ag*., *L. sa*. and *L. av*.) appeared in the top ten enriched species. Many studies on chicken demonstrated that the *Lactobacillus* was the predominant genus in the ileum (Kumar *et al*., 2018). *L. sa*. was present throughout the small intestine, increased in the duodenum, peaked in the jejunum, and decreased in the ileum (Shanmugasundaram *et al*., 2019). Furthermore, growing studies suggested that *Lactobacillus* can regulate mucosal structure and function. For example, *Lactobacillus* were proved to protect the intestinal barrier and activated intestinal epithelial proliferation in mice or humans (Hou *et al*., 2018; Han *et al*., 2019). To further

identify the regulation of *L. ag*., *L. sa*. and *L. av*. on the intestinal mucosa of laying hens, the HL Hens (with fewer villus wrinkles) were fed with *L. ag*., *L. sa*. and *L. av*. singly or combined for 30 consecutive days, and found that the villus wrinkles amount and the villus circumference (absorption area) were remarkably increased after co-feeding of *L. sa*. and *L. ag*. Therefore, we speculated that the increased villus wrinkles were due to the enhancing of epithelial proliferation. Consistently, our study further showed that mucosal PCNA expression *in vivo* and organoids EdU incorporation *in vitro* could be up-regulated under *L. sa*. + *L. ag*. treatment. Similarly, *L. reuteri 22* fed in young chicken was demonstrated to enhance intestinal mucosal PCNA expression (Xie *et al*., 2019). Taken together, we propose that *L. sa*., *L. ag*. and *L. av*. were critical for the formation of unique intestinal morphology in ZN Hens at the laying peak period, especially for the combination of *L. sa*. and *L. ag*.

Previously, the *L. sa*. and *L. fermentum* co-feeding in DSS-mouse colitis could restore the intestinal microbiota homeostasis and modulate the immune response (Rodríguez-Nogales *et al*., 2017). In this study, *L. sa*. + *L. ag*. feeding could remarkably up-regulate many probiotics species in HL Hens, such as *Bifidobacterium*, *C. butyricum*, *L. casei*, etc. Simultaneously, *L. sa*. + *L. ag*. feeding could decrease pathogenic microorganism abundance, such as *C. disporicum*, which was first isolated from rat intestinal flora in 1987 and associated with Crohn's disease patients in humans (Mangin *et al*., 2004). It also confirms the results of PCoA (Fig. 3E) and NMDS (Fig. 3F) that a significant separation in bacterial community composition existed among the three laying periods in ZN Hens, which were clustered at the high abundance of probiotics (Fig. 4). Consistent with this result, the co-feeding of *L. sa*. and *L. ag*. in chicken was demonstrated to increase the count of *L. ag*., reduce the number of *Enterobacteriaceae*, and finally increased weight gains (Lan *et al*., 2003). Furthermore, feeding of *L. casei* in humans could increase the relative abundance of lactic acid bacteria in the gut while inhibiting the growth of certain harmful bacteria (Hou *et al*., 2020). Additionally, the dietary restriction could alleviate the Methotrexate-induced intestinal injury in mice by increasing the intestinal *Lactobacillus* genus (Tang *et al*., 2020). These were indicating that feeding *L. sa*. + *L. ag*. could effectively improve intestinal microbial communities and reduce the stimulation of pathogenic bacterium on intestinal mucosa.

Multiple studies have shown that probiotics could increase the amount of $Lgr5^+$ ISCs and further increase the villi height, crypt depth, mucosa thickness, and the amount of Paneth cells and goblet cells in the small intestine of mice (Hou *et al*., 2018; Lee *et al*., 2018). In contrast, the activity of ISCs could also be up-regulated under the pathogenic microorganism infection, such as *Salmonella Pullorum* challenge (Xie *et al*., 2019). In our study, the activity of ISCs *in vitro* could be enhanced by *L. sa*. + *L. ag*. treatment. However, crypt's Lgr5 levels decreased dramatically after *L. sa*. + *L. ag*. feeding in HL Hens, it would be the result of improved intestinal microbial communities caused weak stimulation of pathogenic microorganisms to ISC. Thus, we speculate that *L. sa*. + *L. ag*. feeding in HL Hens could indirectly fine modulate the ISCs activity *in vivo* through intestinal microbiota.

In conclusion, we suggested that the co-feeding of *L. sa*. and *L. ag*. in laying hens could effectively improve the intestinal microbial community composition, increase the abundance of probiotics, in turn, promote epithelial proliferation, finally, increase villus wrinkles amount and the villus absorption area. Next step, how do the probiotics regulate the ISCs activity of laying hens, is worthy of being investigated.

Experimental procedures

Animals

ZN Hens and HL Hens were purchased from commercial chicken farms at the age of 150-day-old (D150, pre-laying peak period), 280-day-old (D280, laying peak period) and 580-day-old (D580, post-laying peak period) respectively. All birds were raised conventionally for further study (stocking density was 675 cm^2 per bird, fed with the basal diet and free access to water, temperature maintained at 15–20°C). The composition of the basal diet is shown in Table S2. This study was carried out following the *Guiding Principles for the Care and Use of Laboratory Animals of Zhejiang University*. The experimental protocols were approved by the *Committee on the Ethics of Animal Experiments of Zhejiang University* (No.: 18315).

Multiple-antibiotics feeding

To prove intestinal flora regulation on mucosal structure, 12 D280 ZN Hens were divided into two groups, one control and one multiple-antibiotic feeding group. In the control group, hens were fed with a basal diet and free access to water. However, in the multiple-antibiotics group, hens were supplied with water containing Ampicillin Sodium (1 g l^{-1} water, MB1378; Meilunbio, Dalian, China), Neomycin Sulfate (1 g l^{-1} water, MB1716; Meilunbio), Metronidazole (1 g l^{-1} water, MB2200; Meilunbio, Dalian, China) and Vancomycin HCl (0.5 g l^{-1} water, MB1260; Meilunbio) for five consecutive days. On the sixth day, all the hens were killed after anaesthesia. The gut lumen content was then collected sterilely,

further used for Colony-Forming Units (CFUs) counting and 16S rRNA gene sequencing. Meanwhile, the intestinal tissue and intestinal crypt were collected for morphology, mRNA transcription and protein expression assays.

Lactobacillus *feeding trial*

Lactobacillus salivarius (CGMCC 1.1881), *L. ag.* (CGMCC 1.3914) and *L. av.* (CICC 20991) were purchased from the China General Microbiological Culture Collection Centre (CGMCC) or China Centre of Industrial Culture Collection (CICC), and cultured in MRS broth (Beijing Land Bridge Technology Co., CM187, Beijing, China) at 37°C overnight in aerobic conditions. The cultured bacteria were harvested by centrifugation (4500 *g*) and adjusted with 5% skim milk to obtain a final concentration of 10^8 CFUs ml^{-1}. The bacterial suspension was stored at −80°C until use.

The HL Hens at the age of D280 were raised in a commercial chicken farm and then randomly divided into seven groups ($n = 6$), one control group and six *Lactobacillus* feeding groups. In the control group, hens were fed with a basal diet and free access to water. The six *Lactobacillus* feeding groups were, respectively, supplied with basal diet containing *L. sa.*, *L. ag.*, *L. av.*, *L. sa.* + *L. ag.*, *L. sa.* + *L. av.* and *L. ag.* + *L. av.* The final concentration of *Lactobacillus* in each group is 10^8 CFUs/hen/day and fed for 30 consecutive days.

Morphological assay

The duodenum, jejunum and ileum were collected and cleaned using PBS (pH 7.4), then fixed in 4% paraformaldehyde (PFA, pH 7.4) or liquid nitrogen until analysing. For analysing mucosal morphology, hematoxylin & eosin (H&E) staining and alcian blue-periodic acid Schiff (AB-PAS) reactions were performed according to the conventional histological procedures. Fifty intact villi in each group were used to analyse the goblet cell density (amount/100 μm villus length, referred to Li *et al.*, 2017).

Protein expression assay

For analysing the expression of Lgr5 (a marker of ISCs) and PCNA (a marker of proliferation cells) in the duodenum and crypt organoids, Immunohistochemistry (IHC), Immunofluorescence (IF) and Western Blot (WB) were performed. Briefly, for IHC/IF, the intestinal section samples were incubated with rabbit anti-Lgr5 (1:50; HuaBio, customisation, Hangzhou, China) or mouse anti-PCNA (1:200; Abcam, ab29, Cambridge, UK) overnight at 4°C, then incubated with fluorescein isothiocyanate conjugated goat anti-rabbit secondary antibody (1:500; HuaBio, HA1001) or horseradish peroxidase (HRP) conjugated goat anti-mouse secondary antibody (1:500; HuaBio, HA1006) for 1 h at 37°C. For WB, total proteins were extracted from the duodenal crypt and crypt organoids. After SDS-PAGE separating, transferring to polyvinylidene fluoride membrane and skimmed milk blocking. The samples were incubated with rabbit anti-Lgr5 (1:250) or rabbit anti-β-actin (1:50 000; Abclonal, AC026, Wuhan, China) overnight at 4°C, followed by incubation with the HRP-conjugated goat anti-rabbit (1:2000; Abclonal, AS014). For the semiquantitative assay, images were quantified and analysed using the Gel-Pro software, and the grey analysis of target protein bands was normalised with β-actin.

Crypt isolation and organoids culture

Isolation of chicken's intestinal crypt was performed base on the protocol previously published (Li *et al.*, 2018). Briefly, the duodenum was collected from HL Hens in D280 (laying peak period) sterility, cut into 2–4 mm^3 pieces and shaken gently in 2 mM cold EDTA (ethylenediaminetetraacetic acid, pH 7.4). After passing through a 70-μm nylon cell strainer (Corning Inc., 352360; Corning, NY, USA), the crypts were purified by centrifugation (100 *g*) and re-suspended. The purified crypt was further used for mRNA transcription assay, protein expression assay and organoids culture.

The sterilely purified crypts were mixed with Matrigel (354277; Corning), dropped into 24-well flat-bottom plate and administered with a complete culture medium (the advanced DMEM/F12 culture medium comprising 50 ng ml^{-1} EGF, 100 ng ml^{-1} Noggin and 500 ng ml^{-1} R-spondin 1). All these wells were divided into four groups (Control, *L. sa.* + *L. ag.*, *L. sa.* + *L. av.* and *L. ag.* + *L. av.*) and cultured at 37°C in a 5% CO_2 atmosphere for 48 h. The dosage of *Lactobacillus* treatment was 10^4 CFUs per well (referred to Hou *et al.*, 2018). For EdU incorporation assay, EdU reagent (final concentration was 10 μM, MA0425, Meilunbio) was added into the culture medium and incubated for 2 h at 37°C, after fixing by 4% PFA and rinsing by 0.5% Triton in PBS, the samples were reacted with reaction buffer (prepared according to the product manual) for 30 min, then counterstained the nucleus with Hoechst 33342. Meanwhile, the crypt organoids were spun down after dissolving Matrigel by Cell Recovery Solution (354253; Corning), and further used for WB and qPCR analysis.

Quantification Real-Time PCR (qPCR)

Total RNA from the intestinal tissue, intestinal crypt and organoids were extracted using TRIzol reagent and reverse transcribed into cDNA using the SuperScript

Table 1. Primers for PCR analysis.

Genes	Accession No.	Primer sequences (5′–3′)	Product (bp)
MUC2	NM_001004414.2	TACTTCACCTTCAACCATTACAAC CATAGTCACCAC*CAT*CTTCTTCA	119
PepT1	NM_204365	GATCACTGTTGG*CAT*GTTCCT *CAT*TCG*CAT*TGCTATCACCTA	146
B^0AT	XM_419056	AATGGGACAACAAGGCTCAG CAAGATGAAGCAGGGGGATA	165
$b^{0,+}AT$	NM_001199133	TATTTCACCGTAATGACTTCAAC AGGCCACAAAGAGAGGTATTA	112
EAAT3	XM_424930	AAAATGGGAGACAAAGGACAA ACGAAAGATTTCCCAGTCCTC	159
Wnt3a	NM_001171601.1	CTTCTTCAAGGCTCCGACTG GGCACTTCTCTTTCCGTTTC	200
GAPDH	NM_204305	GATGGGTGTCAACCATGAGAAA CAATGCCAAAGTTGTCATGGA	116

First-Strand Synthesis System (11904018; ThermoFisher Scientific, Waltham, MA, USA). The qPCR was carried out on an Applied Biosystems™ 7500 Real-Time PCR machine (ThermoFisher Scientific) with 2 μl cDNA template, 400 nM of each primer (Table 1), 0.4 μl Rox reference dye II, 10 μl SYBR Premix Ex Taq (TaKaRa, Bio Inc., Shiga, Japan) and 6.8 μl water in a total volume of 20 μl. The qPCR conditions were as follows: 95°C for 10 min, and then 40 cycles of 95°C for 30 s, 60°C for 34 s and 72°C for 30 s. All samples were measured in triplicate, and the experiments were repeated more than three times. All samples were normalised with *GAPDH* using the comparative cycle threshold method ($2^{-\Delta\Delta Ct}$).

Intestinal flora sequencing

The small intestinal content of six hens in each group was collected sterilely and frozen in dry-ice and mailed to a commercial company (Novogene Co. Ltd, Beijing, China) for 16S rRNA gene V3-V4 region sequencing. Briefly, DNA was extracted from small gut lumen content using the Qiagen QIAamp DNA Stool yMini Kit (Qiagen, Hilden, Germany) according to the protocol, followed by PCR amplified using bar-coded primers flanking the V3-V4 region of the 16S rRNA gene. Amplicons were extracted from 2% agarose gels, purified using the Axy-Prep DNA Gel Extraction Kit (Axygen Biosciences, Union City, CA, USA), then pooled in equimolar and paired-end sequenced (2 × 250) on an Illumina MiSeq platform. Raw fastq files were demultiplexed and quality-filtered using QIIME (http://qiime.org/). Operational taxonomy units (OTUs) were clustered with 97% similarity cut-off using UPARSE (version 7.1 http://drive5.com/uparse/), and chimeric sequences were identified and removed using UCHIME. The taxonomy of each 16S rRNA gene sequence was analysed by the RD *P*-value < Classifier (http://rdp.cme.msu.edu/) against the silva (SSU115) 16S rRNA gene database using the confidence threshold of 70%. The representative sequences of OTUs and their relative abundance were used to calculate the rarefaction analysis. QIIME was used for analysing α-diversity and β-diversity. The α-diversity analysis includes calculating the observed species, Chao 1 and Shannon indices. The β-diversity analysis includes principal coordinate analysis (PCoA) and nonmetric multidimensional scaling (NMDS). The predominant bacterial community difference between groups was detected using the LDA effect size.

Statistical analysis

Statistical analyses were performed using SPSS 16.0 (SPSS Inc., Chicago, IL, USA). For normally distributed data, t-test and one-way analysis of variance (ANOVA, followed by the Least Significant Difference post hoc multiple comparison test) was carried out. For non-parametric analysis, Kruskal-Wallis test was performed to analyse the statistical significance among various groups, followed by the pairwise-Wilcoxon test (with *P*-value adjusted by FDR method of Benjamini and Hochberg). The significance level was set at P-value < 0.05.

Acknowledgements

This study was supported by the National Natural Science Foundation of China (No. 31972630) and the Zhejiang Provincial Basic Public Welfare Research Program (No. LGN21C180003). We are grateful to Weidong Zeng (Zhejiang University) and the Experimental Teaching Centre (College of Animal Sciences, Zhejiang University) for help in the experiments.

Funding Information

This study was supported by the National Natural Science Foundation of China (No. 31972630) and the

Zhejiang Provincial Basic Public Welfare Research Program (No. LGN21C180003).

Conflict of interest

The authors declare that they have no conflict of interest.

Author contributions

L.J. Liu and Z. Zhou conducted the experiments, collected and analysed the data, and wrote the manuscript. Y. Hong, K.Y. Jiang, L.Z. Yu and X.C. Xie were responsible for the animal experiments. Y.L. Mi, S.J. Zhu and C.Q. Zhang were responsible for data interpretation and manuscript revision. J. Li was responsible for the conception and design of the study, analysis and interpretation of data, and final approval of the version submitted. All authors reviewed the manuscript.

References

Abdelqader, A., Al-Fataftah, A.R., and Daş, G. (2013) Effects of dietary *Bacillus subtilis* and inulin supplementation on performance, eggshell quality, intestinal morphology and microflora composition of laying hens in the late phase of production. *Anim Feed Sci Technol* **179:** 103–111.

Athiyyah, A.F., Darma, A., Ranuh, R., Riawan, W., Endaryanto, A., Rantam, F.A., *et al*. (2018) *Lactobacillus plantarum* IS-10506 activates intestinal stem cells in a rodent model. *Benef Microbes* **9:** 755–760.

Gu, Y.F., Chen, Y.P., Jin, R., Wang, C., Wen, C., and Zhou, Y.M. (2021) A comparison of intestinal integrity, digestive function, and egg quality in laying hens with different ages. *Poult Sci* **100:** 100949.

Han, X., Lee, A., Huang, S., Gao, J., Spence, J.R., and Owyang, C. (2019) *Lactobacillus rhamnosus* GG prevents epithelial barrier dysfunction induced by interferon-gamma and fecal supernatants from irritable bowel syndrome patients in human intestinal enteroids and colonoids. *Gut Microbes* **10:** 59–76.

Hou, Q.H., Ye, L.L., Liu, H.F., Huang, L.L., Yang, Q., Turner, J.R., and Yu, Q.H. (2018) *Lactobacillus* accelerates ISCs regeneration to protect the integrity of intestinal mucosa through activation of STAT3 signaling pathway induced by LPLs secretion of IL-22. *Cell Death Differ* **25:** 1657–1670.

Hou, Q., Zhao, F., Liu, W., Lv, R., Khine, W.W.T., Han, J., *et al*. (2020) Probiotic-directed modulation of gut microbiota is basal microbiome dependent. *Gut Microbes* **12:** 1736974.

Hu, J., Ma, L., Nie, Y., Chen, J., Zheng, W., Wang, X., *et al*. (2018) A microbiota-derived bacteriocin targets the host to confer diarrhea resistance in early-weaned piglets. *Cell Host Microbe* **24:** 817–832.

Kumar, S., Chen, C.X., Indugu, N., Werlang, G.O., Singh, M., Kim, W.K., and Thippareddi, H. (2018) Effect of antibiotic withdrawal in feed on chicken gut microbial dynamics, immunity, growth performance and prevalence of foodborne pathogens. *PLoS One* **13:** e0192450.

Lan, P.T.N., Binh, L.T., and Benno, Y. (2003) Impact of two probiotic *Lactobacillus* strains feeding on fecal lactobacilli and weight gains in chicken. *J Gen Appl Microbiol* **49:** 29–36.

Lee, Y.-S., Kim, T.-Y., Kim, Y., Lee, S.-H., Kim, S., Kang, S.W., *et al*. (2018) Microbiota-derived lactate accelerates intestinal stem-cell-mediated epithelial development. *Cell Host Microbe* **24:** 833–846.e6.

Li, J., Li, J. Jr, Zhang, S.Y., Li, R.X., Lin, X., Mi, Y.L., and Zhang, C.Q. (2018) Culture and characterization of chicken small intestinal crypts. *Poult Sci* **97:** 1536–1543.

Li, J., Li, R.X., Liu, G., Lv, C.F., Mi, Y.L., and Zhang, C.Q. (2017) Effect of melatonin on renewal of chicken small intestinal mucosa. *Poult Sci* **96:** 2942–2949.

Lokapirnasari, W., Al Arif, A., Soeharsono, S., Fathinah, A., Najwan, R., Pramuda Wardhani, H.C., *et al*. (2019) Improves in external and internal egg quality of Japanese quail (*Coturnix coturnix japonica*) by giving lactic acid bacteria as alternative antibiotic growth promoter. *Iran J Microbiol* **11:** 406–411.

Mancabelli, L., Ferrario, C., Milani, C., Mangifesta, M., Turroni, F., Duranti, S., *et al*. (2016) Insights into the biodiversity of the gut microbiota of broiler chickens. *Environ Microbiol* **18:** 4727–4738.

Mangin, I.Ã¨NE., Bonnet, R.Ã., Seksik, P., Rigottier-Gois, L., Sutren, M.Ã¨NE., Bouhnik, Y., *et al*. (2004) Molecular inventory of faecal microflora in patient swith Crohn's disease. *FEMS Microbiol Ecol* **50:** 25–36.

Metzler-Zebeli, B.U., Magowan, E., Hollmann, M., Ball, M., Molnár, A., Witter, K., *et al*. (2018) Differences in intestinal size, structure, and function contributing to feed efficiency in broiler chickens reared at geographically distant locations. *Poult Sci* **97:** 578–591.

O'Hara, A.M., and Shanahan, F. (2006) The gut flora as a forgotten organ. *EMBO Rep* **7:** 688–693.

Ribeiro, V., Albino, L.F.T., Rostagno, H.S., Barreto, S.L.T., Hannas, M.I., Harrington, D., *et al*. (2014) Effects of the dietary supplementation of *Bacillus subtilis* levels on performance, egg quality and excreta moisture of layers. *Anim Feed Sci Technol* **195:** 142–146.

Rodríguez-Nogales, A., Algieri, F., Garrido-Mesa, J., Vezza, T., Utrilla, M.P., Chueca, N., *et al*. (2017) Differential intestinal anti-inflammatory effects of *Lactobacillus fermentum* and *Lactobacillus salivarius* in DSS mouse colitis: impact on microRNAs expression and microbiota composition. *Mol Nutr Food Res* **61:** 1700144.

Rubio, L.A., Ruiz, R., Peinado, M.J., and Echavarri, A. (2010) Morphology and enzymatic activity of the small intestinal mucosa of Iberian pigs as compared with a lean pig strain. *J Anim Sci* **88:** 3590–3597.

Schoenborn, A.A., von Furstenberg, R.J., Valsaraj, S., Hussain, F.S., Stein, M., Shanahan, M.T., *et al*. (2019) The enteric microbiota regulates jejunal Paneth cell number and function without impacting intestinal stem cells. *Gut Microbes* **10:** 45–58.

Shang, Y., Kumar, S., Oakley, B., and Kim, W.K. (2018) Chicken gut microbiota: importance and detection technology. *Front Vet Sci* **5:** 254.

Shanmugasundaram, R., Mortada, M., Murugesan, G.R., and Selvaraj, R.K. (2019) In vitro characterization and analysis of probiotic species in the chicken intestine by real-time polymerase chain reaction. *Poult Sci* **98:** 5840–5846.

Tang, D., Zeng, T., Wang, Y., Cui, H., Wu, J., Zou, B., *et al*. (2020) Dietary restriction increases protective gut bacteria to rescue lethal methotrexate-induced intestinal toxicity. *Gut Microbes* **12:** 1714401.

Wu, H.Q., Xie, S., Miao, J.F., Li, Y.C., Wang, Z.H., Wang, M.J., and Yu, Q.H. (2020) *Lactobacillus reuteri* maintains intestinal epithelial regeneration and repairs damaged intestinal mucosa. *Gut Microbes* **11:** 997–1014.

Xie, S., Zhao, S.Y., Jiang, L., Lu, L.H., Yang, Q., and Yu, Q.H. (2019) *Lactobacillus reuteri* stimulates intestinal epithelial proliferation and induces differentiation into goblet cells in young chickens. *J Agric Food Chem* **67:** 13758–13766.

Xu, T.Y., Chen, Y., Yu, L.F., Wang, J., Huang, M.X., and Zhu, N.H. (2020) Effects of *Lactobacillus plantarum* on intestinal integrity and immune responses of egg-laying chickens infected with *Clostridium perfringens* under the free-range or the specific pathogen free environment. *BMC Vet Res* **16:** 47.

Supporting information

Additional supporting information may be found online in the Supporting Information section at the end of the article.

Table S1. Difference of albumen amino acid levels between ZhenNing (ZN) Hens and HyLine (HL) Hens ($n = 5$).

Table S2. Composition and nutrient level of the basal diets.

